

Magnetic properties of the perovskite NdNiO₃: Monte Carlo Study

M.Oumarou, N.Aknin, N.Mohamedou, M.L.Ould Ne

Abstract— In this work, we used Monte Carlo method simulation to study the magnetic properties of the perovskite NdNiO₃ within Blume-Capel model. This perovskite has been modeled by a mixed system with spins (3/2, 1/2). The element Nd³⁺ corresponds to spin-3/2 while the spin-1/2 corresponds to the Ni³⁺ one. We found that the stable phases correspond to the configurations: (+3/2, +1/2), (-3/2, 1/2), (1/2, -1/2), and (1/2, 1/2). Moreover, we studied the phase diagram for ground state at T=0 in the plans (r₁, r₂), (r₁, Δ), (r₁, h) and (r₂, h), (r₂, Δ), (Δ, h) with r₁ and r₂ are coupling interaction between Nd-Nd and Ni-Ni respectively, h is the external field and Δ is the crystal field and for a different values of the latest size from N=2 to 14 of the system, r₁=JNd-Nd/JNd-Ni, r₂=JNi-Ni/JNd-Ni, d=Δ/JNi-Nd and h=H/JNi-Nd H is the external magnetic field applied over all spins of the crystal in the z direction. It has been found that the exchange interaction r₁ increase by increase the value of TC (critical-Temperature). Furthermore, the hysteresis cycles loops are investigated.

Index Terms— NdNiO₃, Monte Carlo simulations, Magnetic properties, ground state, Blume-Capel model, Ferromagnetic case.

1 INTRODUCTION

Perovskite form one element of the main families of crystalline oxides, the general form is (RENO₃) with RE is Rare Earth. The perovskite name comes from the mineral that has a similar crystal structure as the CaTiO₃. This mineral was first described in 1830 by Gustav Rose geologist and is re-named after that by Russian mineralogist Lev Perovskite [1]. The typical cell of a perovskite has a cubic symmetry, but a major exception is known, they present more adjacent structures or less distorted. The chemical composition of a perovskite structure oxide is most often consisting of an alkaline earth cation (A), a transition cation tetravalent (B) and oxide anions. (A₂B₂VO₆) corresponds to the reference composition CaTiO₃ whose structure is orthorhombic. However, A₂B₂VO₆ and A₂BVO₆ Compositions It has long been known [2]. The crystal lattice parameters of NdNiO₃ a = 5.3891, b = 5.3816 Å, c = 7.6101 Å [2]. And the space group is (No=62, Pbnm). We recall that the phase of NdNiO₃ at T=0 is antiferromagnetic metal-insulator transition. The band gap value is equal to 15 meV and the Curie Temperature is near of 200K and the Neel Temperature is TN=140 [3-4]. Recently, many researchers have made many efforts to study the magnetic properties of materials with different geometric structures [4-6]. For this purpose, The Magnetic properties have been studied by different methods, mean-field approximation (MFA) and Monte Carlo simulations describing ferromagnetic (FM) semiconductors with increased Curie temperature [7-9]. It is clear that many systems have been explored to study the magnetic properties of materials with different geometric structures [10,11]. In fact, a particular emphasis has put on hexagonal configurations [12, 13]. This study was extended to perovskite, being considered as a topic of a great interest in strongly correlated electron systems [14, 15]. Recently, it was found that the ferromagnetic perovskite systems could be exploited in spintronics for next generation. However, most insulating magnetic perovskite are antiferromagnetic (AFM) [13-20]. To get more insight at this problem, a ferromagnetic semiconductor from perovskite oxides have been proposed with four distinct magnetic phases that are non-magnetic (Nm) ferro-

magnetic (FM), antiferromagnetic (AFM) and Ferromagnetic (FM) phase. The survey was conducted using the DFT method based on ab-initio calculations [19].

The aim of this work is to contribute to these activities by studying the magnetic properties of the NdNiO₃ perovskite using Monte Carlo simulations. First, we elaborate the ground state phase diagram. Then, we discuss the thermal behavior of the magnetizations and the susceptibilities of such systems.

2 THE MODEL AND STRUCTURE

Monte Carlo Method is used to study the behavior of complex spin systems, our study consists of two interpenetrating sublattices. One sublattice has spins σ and take the values ± 1 and 0, the other sublattice has spins S that can take four values: ± 2 , 0, and ± 1 . The spins S have only the spins σ as nearest neighbors and vice versa. The interaction between the spins σ and S is assumed to be an antiferromagnetic exchange. The Hamiltonian of the model is written as:

$$\mathcal{H} = -J_{Mn-Mn} \sum_{\langle i,j \rangle} S_i S_j - J_{Pr-Pr} \sum_{\langle i,j \rangle} \sigma_i \sigma_j - J_{Mn-Pr} \sum_{\langle i,j \rangle} \sigma_i S_j - \Delta_1 \sum_i S_i^2 - \Delta_2 \sum_i \sigma_i^2 - H \sum_i (S_i + \sigma_i) \quad (1)$$

With $\langle i, j \rangle$ stand for nearest-neighbors spins, J_{Nd-Nd} is the coupling interaction constant between spins of Nd (S) and Ni (σ). J_{Nd-Nd} and J_{Ni-Ni} denote the coupling interaction constant between spins S-S and $\sigma - \sigma$, respectively, and the magnetic spin moment are $S=3/2$ and $\sigma=1/2$. H is the external magnetic field applied over all spins of the crystal in the z direction and Δ is the crystal field acting on the spins, this field is originated from the competition between Nd-O and Ni-O interactions.

The mixed system contains a spin S (atoms of Nd) and σ (atoms of Ni) as shown in Fig. 1(a). We used the Metropolis Monte Carlo to study the magnetic properties in equilibrium state in contact with a heat bath temperature T. This work used the Hamiltonian given in equation. (1). Moreover we used the periodic conditions. First, we calculate the energy:

$$E_T = \frac{1}{L \times L \times L} \langle H \rangle \quad (2)$$

The magnetizations per site given by:

$$m_\sigma = \frac{2}{L \times L \times L} \langle \sum_i \sigma_i \rangle \quad (3)$$

The total magnetization is calculated by:

$$m_T = \frac{m_\sigma + m_s}{2} \quad (4)$$

The partials and total susceptibilities can be described by:

$$\chi_s = \beta (\langle m_s^2 \rangle - \langle m_s \rangle^2) \quad (5)$$

$$\chi_\sigma = \beta (\langle m_\sigma^2 \rangle - \langle m_\sigma \rangle^2) \quad (6)$$

$$\chi_{tot} = \beta (\langle m_{tot}^2 \rangle - \langle m_{tot} \rangle^2) \quad (7)$$

Where $\beta = \frac{1}{k_B T}$, and k_B is the Boltzmann constant, we fixed $k_B = 1$ simplicity of calculations.

We also calculate the energy of the system per site:

$$E_T = \frac{1}{L \times L \times L} \langle H \rangle \quad (8)$$

The geometry of the studied perovskite structure is displayed in Fig.1. By simulating the model given in Eq. (1). We have carried out a Monte Carlo method in which configurations are generated by sequentially visiting all the spins in the system and free boundary conditions were imposed. Moreover, the flips are accepted or rejected according to a heat bath algorithm under a Metropolis conditions. Therefore, the system gradually achieves equilibrium after first 7000 Monte Carlo step and the data are obtained with 105 Monte Carlo Step per site (MCSS) at each temperature averaging over many initial conditions to compute the physical quantities.

3.1 Results and discussions

In these results, we investigate the phase diagram at zero temperature. Also, we would like to interpret and discuss the thermal behavior of susceptibility and magnetization and affected by both crystal field and external magnetic field on the system, we used the Hamiltonian showed in equation (1). The exchange coupling constants are $r_1=J_2/J_1$, $r_2=J_3/J_1$ and the crystal field $d=\Delta/J_1$, the external magnetic field $h=H/J_1$, the temperature $t=T/J_1$. The stable phases are obtained by minimizing the values of energy for each parameter and for a fixed values of the size in the system.

In this section of this work we will discuss the results obtained first, we study the ground state when the temperature is zero. In order to validate our results, we have plotted magnetizations as a function of r with different values to confirm the appearance of each phase in the phase diagram. As it seen in figure 2.

On the other hand, the effect of sizes on the magnetic properties has been studied. We have plotted magnetization, susceptibility and specific heat for several different values of the size of system, we found for M exhibit a first order transition and decrease with as the value of size is increased, also the peaks of susceptibilities or specific heat is also increasing with the as the size of the system N was increasing. We found the higher of the peak is 8 for the critical temperature, remains constant during change of size And value is 14 as shown in figures 3, 4 and 5. Moreover, To study the effect of exchange interaction r_1 on the system we have plotted the magnetization susceptibility, and specific heat for different values of r_1 with fixed value of $r_2=1$ and $d_1=d_2=1$ and $h=0$, in this case we found the T_c is increased with increasing the value of r_1 figure 11. The effect of the crystal field on the magnetic properties, we have been presented the magnetization as a function of crystal field (d) with different values of r_1 we found two phases antiferromagnetic and ferromagnetic for a reduced value $r_1=-2$, $r_2=-1$ (Negative part) and $r_1=1$, $r_2=2$ (Positive part), respectively, we presented the hysteresis cycles as a function external magnetic field h, this figure is plotted with different values of T. In this case the values of coercive field h_c change depending on the temperature.

Finally, We observe that remnant magnetization decrease as the coercive field increase.

3.2 Figures Captins:

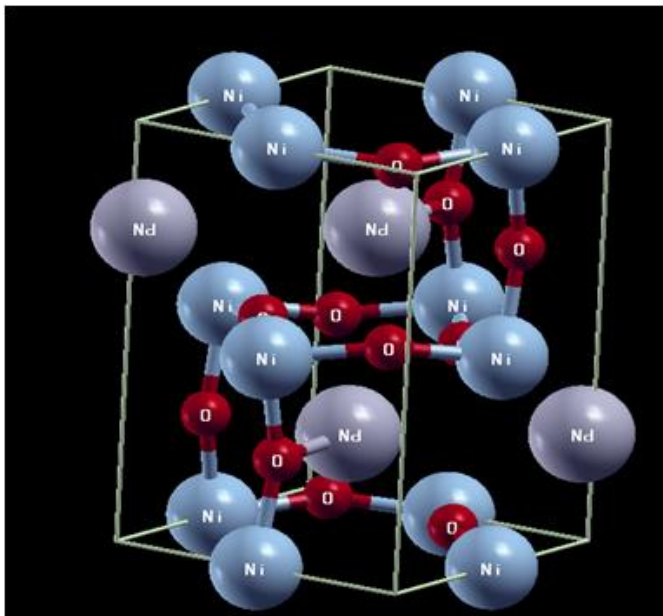


Fig 1

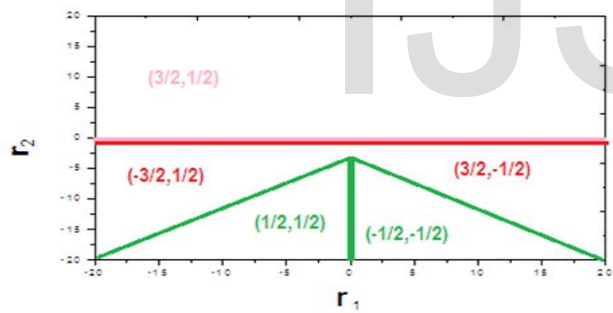


Fig 2.(a)

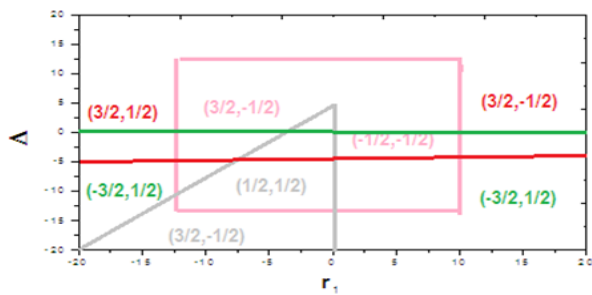


Fig2.(b)

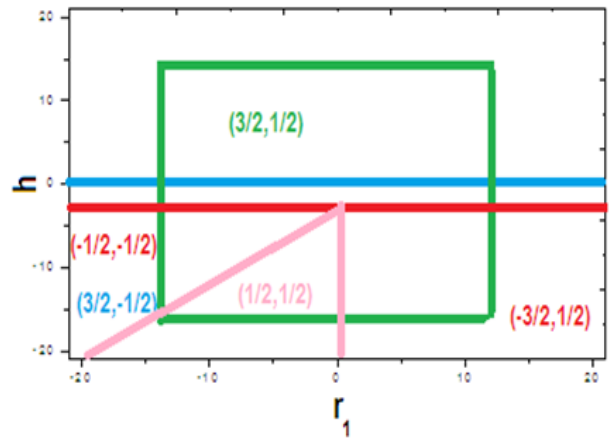


Fig2.(c)

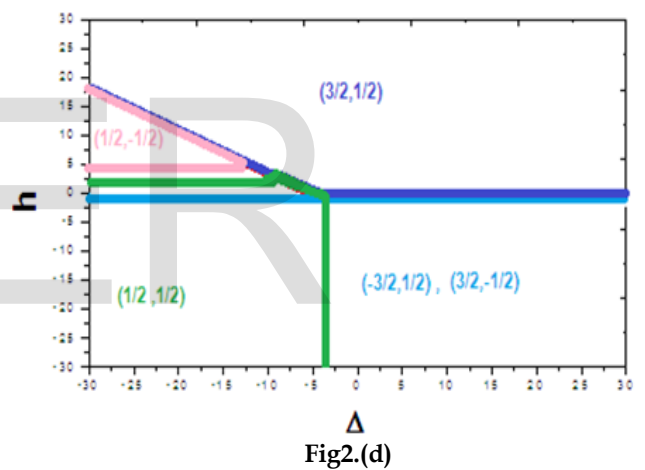


Fig2.(d)

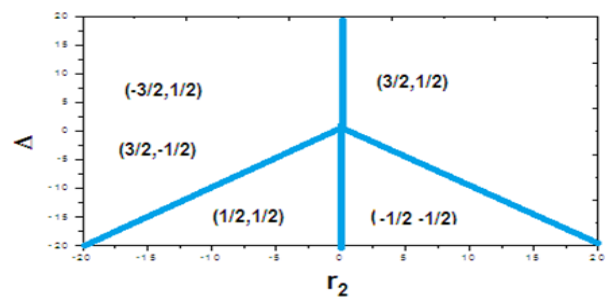


Fig2.(e)

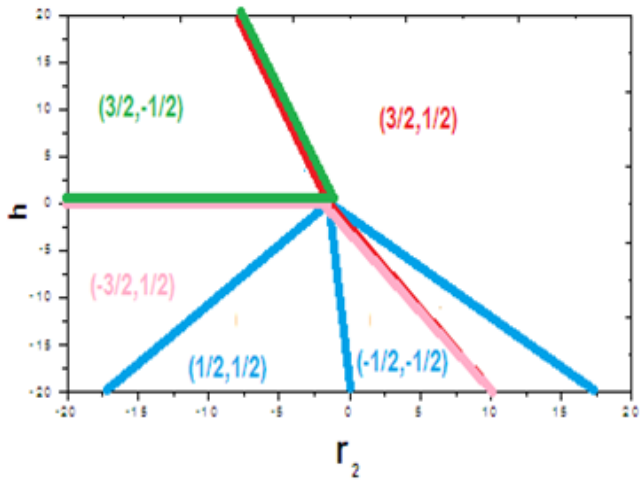


Fig2.(f)

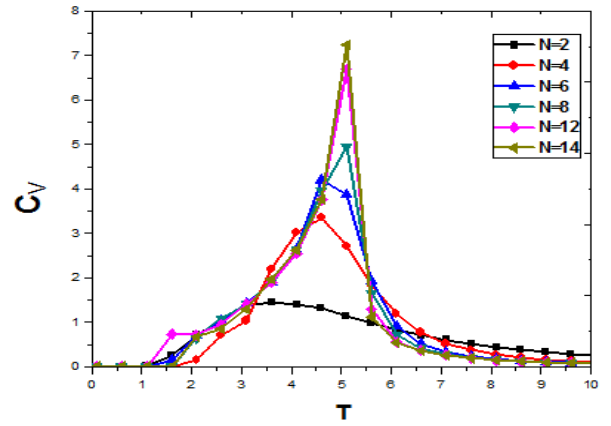


Fig5

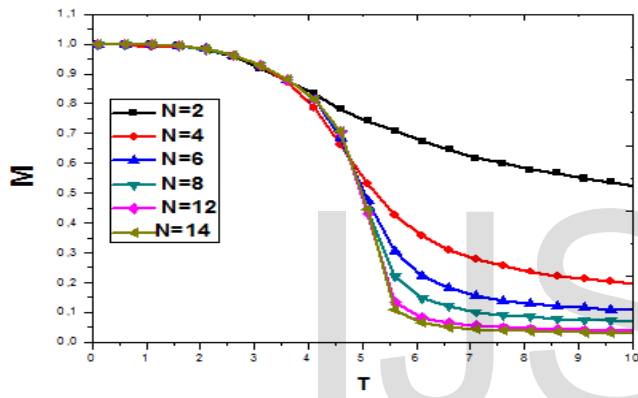


Fig3

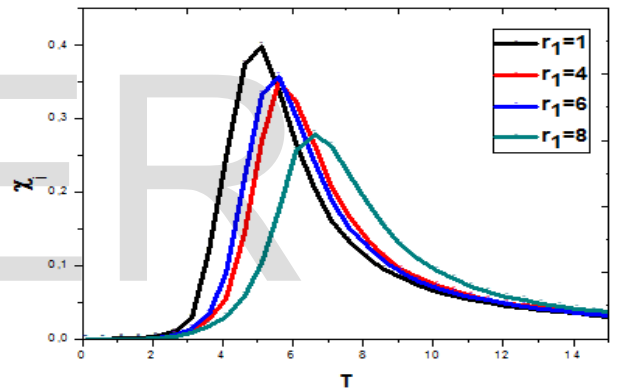


Fig6

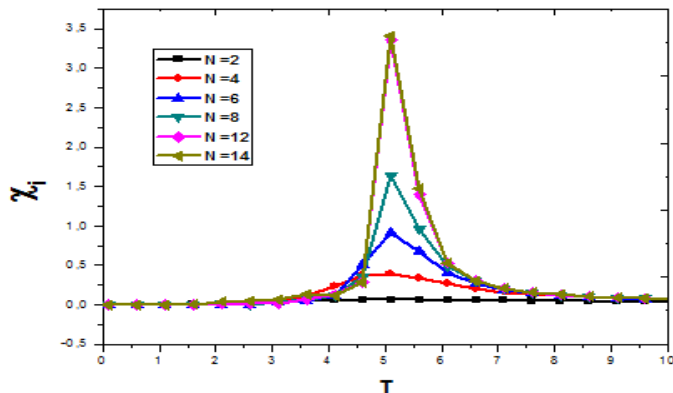


Fig4

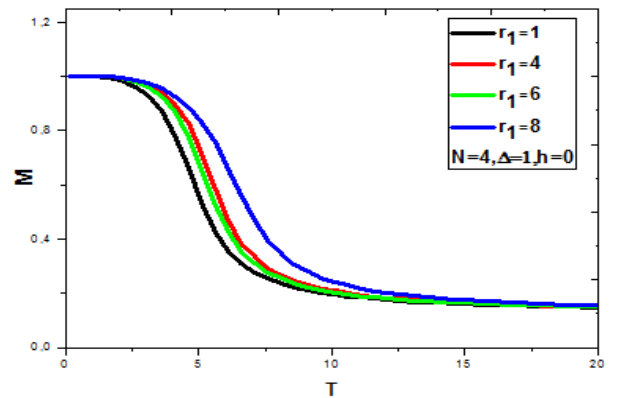
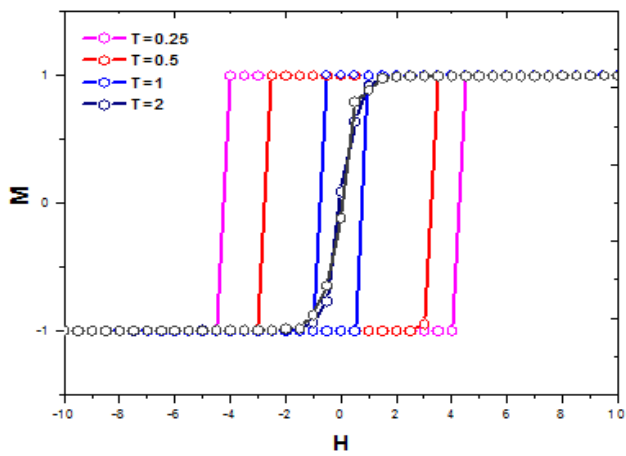
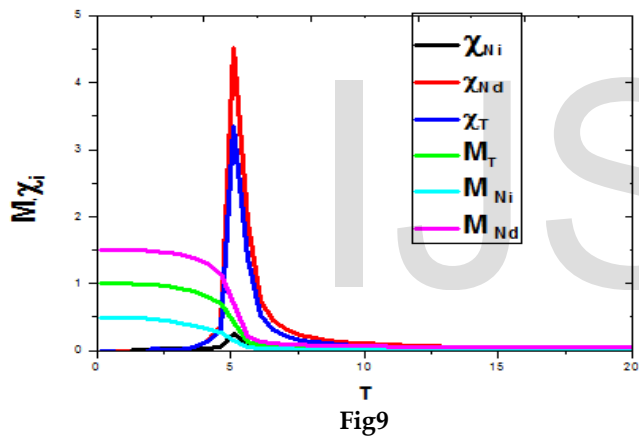
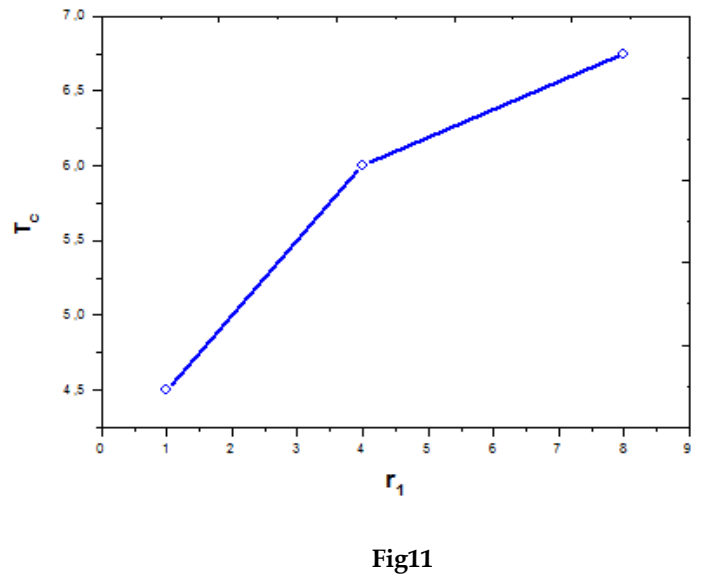
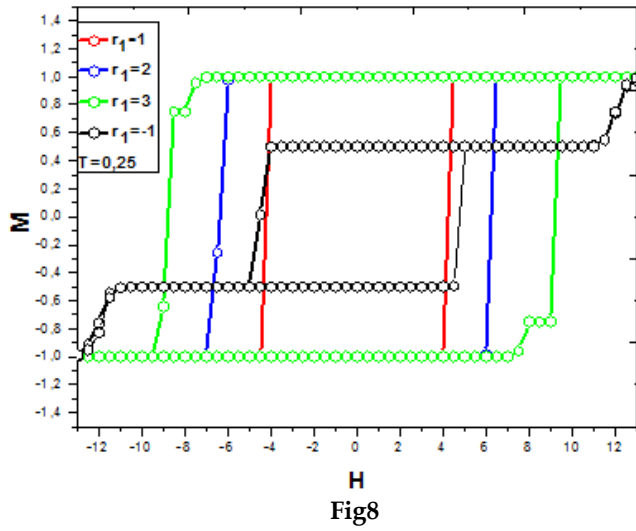


Fig7



3.3 List of Figures :

Fig.1.The geometry structure of NdNiO₃.

Fig. 2. The ground state phase diagrams in different planes showing different configurations: (a) in the plane (r₂, r₁), (b) in the plane (Δ, r₁). (c) In the plane (h, r₁). (d) In the plane (h, Δ), (e) In the plane (Δ, r₂), and (e) In the plane (h, r₂).

Fig. 3. The total magnetization as a function of temperature for various value of size of the system from N= 2, to 14. With fixed value of coupling interaction r₁=r₂=1.0; in the absence of the external magnetic field h=0.0 and crystal field d=1.0.

Fig. 4.The total susceptibility Xi, as a function of temperature for various value of size of the system from N= 2, to 14. With fixed value of coupling interaction r₁=r₂=1.0; in the absence of the external magnetic field h=0.0 and crystal field d=1.0.

Fig. 5.The total specific heat Cv function of temperature for various value of size of the system from N= 2, to 14. With fixed value of coupling interaction r₁=r₂=1.0; in the absence of the external magnetic field h=0.0 and crystal field d=1.0.

Fig.6. The total susceptibility as a function of temperature for various value of coupling interaction r₁=1, 4, 6,8 and fixed coupling interaction r₂=1 with absence value of extern field h.

Fig.7.The magnetization as a function of temperature for various value of coupling interaction r₁=1, 4, 6, 8 and fixed coupling interaction r₂=1, crystal field d=1.0, and value of size of the system N=4 with absence value of extern field h.

Fig. 8. The total magnetization versus the reduced external magnetic field for different reduced exchange coupling interaction values r₁=1,2,3,-1; for a fixed reduced exchange coupling interaction value r₂=1, in the absence of the external magnetic field h=0.0 and a fixed reduced temperature t= 0.25 .

Fig. 9. The total and partial magnetization, susceptibility as a function of temperature for a fixed reduced exchange interaction value r₁= r₂=1.0, in the absence of the external magnetic field h=0.0 and crystal field d₁=d₂=1.

Fig. 10. The total magnetization as a function of the extern magnetic field with various temperature for different value of temperature t=0.25, 0.5, 1, and 2. And f r₁=r₂=1 and absence value of extern field h=0.

Fig. 11.The critical temperature Tc as a function of coupling interaction r₁ for a fixed value of coupling interaction r₂=1.0, in the absence of the external magnetic field h=0.

4 CONCLUSIONS

In this work, we have studied the magnetic proprieties of the double perovskite NdNiO₃ by exploiting Monte Carlo simulation. First, we have calculated the ground state phase diagrams in plane (r₁,r₂). Among others, we have shown that the only stable configurations in this diagram are: (-3/2,1/2) (3/2,-1/2) and (3/2,1/2). Then, we have discussed the thermal behavior of the magnetizations and the susceptibilities of such system in the ferromagnetic case. Finally, we found that when the exchange coupling increases the critical temperature also increases. The hysteresis cycle loops have also been studied.

REFERENCES

- [1] G.H. Jonker, J.H. Van Santen, *Physica* 16 (1950) 337–349.
- [2] G Demazeau, A. Marbeuf, M. Pouchard and P.Hagenmuller, *J.solidchem*3 (1971) 582
- [3] C. Zener, *Phys. Rev.* 82 (1951) 403–405.
- [4] E. O. Wollan, W. C. Koehler, *Phys.Rev.*100 (1955) 545–563.
- [5] Gupta, A. et al. *Appl. Phys. Lett.* 67 (1995) 3494–3496.
- [6] Y. Wua and H. Chen, *J. Magn. Magn.Mater.*324 (2012) 2153.
- [7] C. Liu, J. Ma and H. Chen, *RSC advances*, 2 (2012), 1009.
- [8] B. Khalil, H. Labrim, O. Mounkachi, B. Belhorma, A. Benyoussef, A. El Kenz, and E. Ntsoenzok, *J. Supercond. Nov. Magn.* 25, (2012),1145.
- [9] D. Gatteschi, O. Kahn, J. S. Miller, F. Palacio, NATO ASI E 198, Plenum, (1991).
- [10] J. L. García-Muñoz Institut de Ciència de Materials de Barcelona, CSIC.
- [11] P. Weiss, *J. Phys. Radium* 6, (1907) 661
- [12] H. E. Stanley, UK, Oxford University Press, (1971).
- [13] K. Binder, P.C. Hohenberg, *Phys. Rev. B* 9 (1974) 2194.
- [14] M. El Yadari, L. Bahmad, A. El Kenz, A. Benyoussef, *Physica A* 392 (2013) 673.
- [15] S. Naji, A. Belhaj, H. Labrim, L. Bahmad, A. Benyoussef and A. El Kenz. *Physica A* 399, (2014) 106
- [16] S. Naji, A. Belhaj, H. Labrim, L. Bahmad, A. Benyoussef, A. El Kenz, *Acta Physica Polonica Series B.* 45 (2014) 947.
- [17] A. Jabar, A. Belhaj, H. Labrim, L. Bahmad, N. Hassanain and A. Benyoussef, *Superlattices and Microstructures*, 78 (2015) 171.
- [18] S. Naji, A. Belhaj, H. Labrim, A. Benyoussef, A. El Kenz, *Eur. Phys. J. B* 85 (2012) 1.
- [19] S. Naji, A. Belhaj, H. Labrim, M. Bhihi, A. Benyoussef and A. El Kenz, *J. Phys. Chem. C* 9, (2014) 4924.
- [20] M. Bowen et al., *Appl. Phys. Lett.* 82 (2003) 233.
- [21] H. Chiba, T. Atou, Y. Syono, *J. Solid State Chem.* 132 (1997) 139.
- [22] L. Bufaiçal, L. Mendonça Ferreira, R. Lora-Serrano, O. Agüero, I. Torriani, E. Granado, P.G. Pagliuso, A. Caytuero, E. Baggio-Saitovich, *J. Appl. Phys.* 103 (2008) 07F716.
- [23] M. Uhl, Samir F. Matar, Bruno Siberchicot, *J. Magn. Magn.Mater.*187 (1998) 201.
- [24] M. Yadari, L. Bahmad, A. Benyoussef and A. El Kenz. *Physica A* 399, (2014) 106.
- [25] Huei-Ru Fuh, Ke-Chuan Weng, Yun-Ping Liu, Yin-Kuo Wang, *Journal of Alloys and Compounds* 622 (2015) 657.
- [26] M. Yadari, L. Bahmad, A. El Kenz and A. Benyoussef, *Journal of Alloys and Compounds* 579 (2013) 86.